Numerical results of modal coupling in the UPMSat-2 structure

Andrés García-Pérez*, Marcos Chimeno Manguán**, Ángel Sanz-Andrés* and Gustavo Alonso*

*Instituto Universitario de Microgravedad "Ignacio Da Riva" (IDR/UPM), Escuela Técnica Superior de Ingeniería Aeronáutica y del Espacio (ETSIAE), Universidad Politécnica de Madrid

Pza. Cardenal Cisneros 3, 28040 Madrid, Spain

andres.garcia.perez@upm.es, angel.sanz.andres@upm.es, gustavo.alonso@upm.es

** Escuela Técnica Superior de Ingeniería Aeronáutica y del Espacio (ETSIAE), Universidad Politécnica de Madrid (UPM)

Pza. Cardenal Cisneros 3, 28040 Madrid, Spain

marcos.chimeno@upm.es

Abstract

This work presents a study of the effects of modal coupling on the microsatellite UPMSat-2, where some design parameters are modified to achieve different levels of modal coupling. The finite element model (FEM) of the satellite is used to obtain the numerical results such as natural frequencies, interface forces and stresses resulted from the different configurations. The results show an appreciable reduction of the forces and stresses on the main structure when the degree of modal coupling is higher. However, the negative effect is the increase of the stresses on the secondary parts, which can overpass their allowable limits.

1. Introduction

For the design of new structures subjected to dynamic loads, it is an indispensable task the evaluation of their modal behaviour in order to predict their response against the different type of mechanical environment [1,2]. One of the most interesting aspects related to the dynamic behaviour of a complex system is the influence, in modal terms, of a secondary part on the entire system in case of modal coupling. The effects of the modal coupling have been studied in the concept of tuned mass dampers (TMD), where the objective is the reduction of the levels of displacements, accelerations, stresses and forces on the main structure by adding a secondary dynamic subsystem that will be exposed to high levels of acceleration and local stresses [3]. In this case, the secondary part must be designed to withstand this intense mechanical environment to prevent its collapse. The TMD concept has been applied in the development of devices that reduce the adverse effects of earthquakes in buildings [4–7]. In these works, the objective is to protect the main structure (building) by adding a dynamic mass-damper system that acts like a secondary part whose fundamental frequency is tuned to be close to the main mode of the primary structure. When a dynamic load is produced exciting these modes, the high motion of the secondary system achieves a significant reduction of the maximum displacements and forces on the primary structure. In these situations, the modal coupling is an intentional effect that improves the protection of the main structure against dynamic loads. However, for other cases, the modal coupling is an undesirable phenomenon that can provoke damages for the sensitive secondary parts. One example is the space systems, where the intense dynamic environment produced during the launch generates high levels of accelerations that are transmitted to all the equipment through the mechanical interfaces. Therefore, with the aim of decreasing the risk of damage caused by the adverse effects of modal coupling on space structures, it is standardized in the space industry the definition by the launcher authorities of requirements that impose a minimum value for the natural frequencies of the spacecraft that will fly on board [2]. With the same purpose, this type of requirement is also derived in the spacecraft projects from the principal contractor of the spacecraft to the different subsystems. In both cases, the secondary subsystem is the affected part that must comply with the imposed requirement to have sufficient guarantee of avoiding the modal coupling, which it is achieved if its natural frequencies are sufficiently higher than the fundamental modes of the primary systems [1]. The problem arises in particular subsystems, such as large telescopes or deployable solar panels, where the design restrictions do not allow to reach the required minimum frequency. This is the case of the telescopes

Andrés García-Pérez, Marcos Chimeno Manguán, Ángel Sanz-Andrés and Gustavo Alonso

for the observation of the cosmos, such as ARIEL mission [8], where its operations require very low temperature that can only be achieved if it is thermally isolated from the rest of the spacecraft. This thermal requirement is fulfilled with a mechanical design that includes isostatic mounts, which have the disadvantage of reducing the main modes of the payload that can lead to the unavoidable coupling with the modes of the main structure. Other cases are the deployable items such as antennas or solar panels [9], which present low modes that must be considered for the attitude dynamics.

In [10], the analytical results obtained from an undamped 2-degree-of-freedom (2-DOF) system quantify these effects. It was demonstrated that, within the range of design parameters where the modal coupling is produced, the main mode of the uncoupled case is transformed into two different modes with similar modal effective mass (MEM) values. This result is always obtained in the 2-DOF system, even for practically negligible mass values for the secondary part, concluding that a small secondary part can significantly influence on the global dynamic behaviour of the entire system. Another interesting effect is the change of the frequencies of both modes for different grades of modal coupling, being more significant with higher secondary–primary mass fractions. Additionally, two design cases were presented in [10], where the equations of the analytical 2-DOF model were developed with the aim of obtaining simple mathematical expressions to get preliminary designs of space systems whose main modes meet the requirements of minimum frequencies in case of modal coupling. These analytical expressions can be useful to estimate the limits imposed to the natural frequencies of secondary subsystems derived from the requirements imposed to the entire system.

In this paper, the phenomenon of modal coupling is numerically investigated with the design of the microsatellite UPMSat-2 [11]. The main lateral modes in the launch configuration of the entire system can be altered by the mechanical design of the communication antennas, which are four thin beams located vertically on top of the satellite and with very small mass compared with the rest of the satellite. Despite the small mass fraction of these secondary elements, the changes on the values of the natural frequencies of the entire system and on their modal effective masses can be significant. The structural responses obtained under a sine vibration environment such as forces and stresses are also modified due to the modal coupling between antennas and main structure. In section 2, a general description of the UPMSat-2 satellite is presented. In sections 3 and 4, the numerical finite element model (FEM) is described and the obtained numerical results are detailed to evaluate the impact of the modal coupling between antennas and satellite on the dynamic behaviour of the entire satellite and on the changes of the structural responses. The design parameters of the antennas are modified to have different grades of modal coupling, what allows the assessment of their influence on the results such as natural frequencies, modal effective masses, interface forces and local stresses. Finally, the conclusions of this work are summarized in section 5.

2. UPMSat-2 description

UPMSat-2 is a microsatellite of 50 kg developed by the research institute Ignacio Da Riva (IDR), which belongs to the Spanish university Universidad Politécnica de Madrid (UPM). The technicians, investigators and professors of the research institute, as well as some students of the engineering schools of aerospace and informatics of UPM, have participated in the design, assembly and testing of this satellite and its equipment, whose main purposes are the space qualification of new technologies, the acquisition of knowledge and experience in the development of a satellite by all participants and the demonstration of the capability of the UPM in the field of space technology [11,12]. Many works have been published related to different aspects of the design and development of the UPMSat-2, such as the design of its magnetic attitude control subsystem [13–15], the design and tests of the power system [16,17] and of the communications subsystem [18]. The UPMSat-2 satellite will be fly to the space together with other small satellites in a multiple payload launch of the Vega in August 2019.

The UPMSat-2 project was conceived with the aim of developing a multipurpose satellite capable of transporting different payloads and performing missions in a variety of scenarios, while the structure and the basic subsystems are simple and with standard designs. With this philosophy, the mechanical design selected for UPMSat-2 is based on its predecessor UPMSat-1, getting a quadrilateral prism structure composed by four horizontal trays, which supports the main payloads, attached laterally at the corners to four L-shape vertical beams and at the side edges to four double-sheet panels (Figure 1). Furthermore, there are a total of eight vertical shear panels located inside between the lower trays, which stiffer the entire structure. All these structural parts are made of the aluminium alloy 7075-T6. This concept was chosen by its simplicity and robustness, with the aim of having a standard design that can be suitable for a wide variety of missions and payloads. Furthermore, the main structure has been designed to withstand the most severe load cases extracted from the mechanical environments defined by a great number of launchers in order to have the possibility of being launched by any of these launch vehicles. Finally, the selected launcher has been Vega.
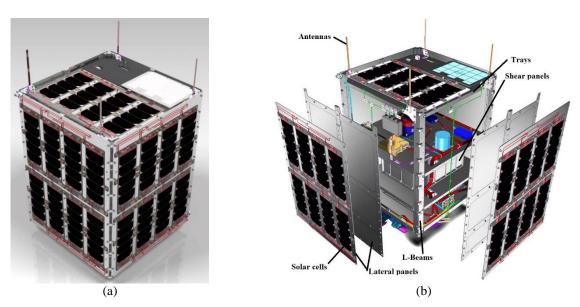
Figure 1: (a) UPMSat-2 CAD design. (b) Structural composition.

At the top of the satellite, four communication antennas are located near the corners, where each one is a thin vertical beam made of a copper – beryllium alloy and clamped by its lower end to the satellite structure. Therefore, each antenna is considered as a vertical cantilevered beam from a mechanical point of view, where the first modes are mainly bending and torsional motions. The dimensions of each antenna in the final design are 167 mm of length, 8 mm of wide and 0.2 mm of thickness, giving a first bending mode of approximately 4 Hz, much lower than the first global mode of the satellite, which is 92 Hz. In this work, the value of the thickness of two opposite antennas is to be modified in the numerical model of the satellite to increase the natural frequency of the local bending modes and therefore, to achieve a higher degree of modal coupling caused by the smaller difference in frequency terms between local and global modes. In this way, the calculated results with the different design configurations will allow the numerical evaluation of the modal coupling between the two antennas and the main structure of the satellite.

3. UPMSat-2 Finite element model

The finite element model (FEM) of the UPMSat-2 are mainly composed by quadrilateral planar elements (QUAD4), which represent the thin-walled structural pieces (Figure 2). Each payload is represented by a point mass attached to the structure by a rigid element, while the mass of the solar cells is taken into account in the model by the non-structural mass (NSM) parameter defined in the elements that represent the external lateral panels. To join the different structural pieces, a set of CBUSH elements together with RBE2 rigid elements has been created to represent the screws that connect these parts. These CBUSH elements allow the calculation of the interface forces that are generated as a result of the application of the different load cases. The antennas are modelled with 1D beam elements located vertically on top of the UPMSat-2 FEM, whose lower ends are attached to the main structure by rigid elements.

The FEM used in this study includes an adaptor under the lower tray of the satellite, which is the mechanical interface between the satellite and the separation system. The boundary conditions of the satellite in the launch configuration are modelled by the constraints of the 6 DOF applied to the lower nodes of the CBUSH elements that represent the bolts between adaptor and separation system. The upper nodes of these CBUSH elements correspond the centre nodes of the RBE2 rigid elements defined in each hole of the adaptor (Figure 3). The results described in this paper have been calculated with this boundary condition in the different proposed analyses.
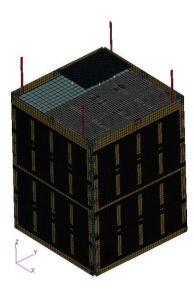
Andrés García-Pérez, Marcos Chimeno Manguán, Ángel Sanz-Andrés and Gustavo Alonso

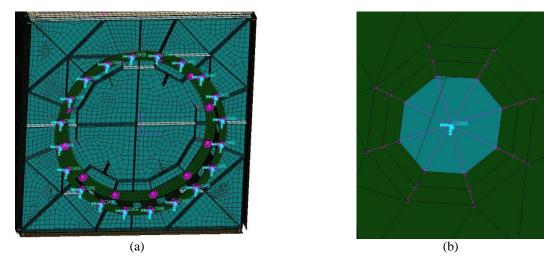Figure 2: Finite element model of UPMSat-2

| (a) | (b) |

Figure 3: (a) FEM of the adaptor and the lower stiffened tray at the bottom face of the UPMSat-2. (b) Detail of the modelling of one interface bolt of the adaptor.

4. Numerical analyses and results

In this section, the results obtained from the normal modes analyses and from the sine vibration simulations with the FEM of the UPMSat-2 are presented, where the thickness of two opposite antennas is modified to have different grades of modal coupling. The selected antennas whose thicknesses will be changed in this study are those in which the thickness direction is perpendicular to the global X-axis. These antennas are located in the corners X+ Y+ and X- Y- (see Figure 2). Therefore, the global mode of interest in this investigation is the main lateral mode of the satellite in X-axis, whose motion is in the same direction as the first bending mode of the selected antennas.

4.1 Normal modes analyses

Some of the numerical results of this work are compared with the analytical solutions of an equivalent 2-DOF model, as the described in [10]. In the development described in [10] for the 2-DOF system, a reference configuration is defined, consisting of the primary structure without the analysed secondary part. Therefore, the first numerical simulation is a normal modes analysis of the FEM of the UPMSat-2 without the two antennas previously mentioned to obtain the reference natural frequency considered in this study. This analysis provides a fundamental natural frequency of the satellite of $f_r = 94.8$ Hz, where the corresponding mode shape can be seen in Figure 4. The mass of the satellite in this reference configuration is 45.950 kg.
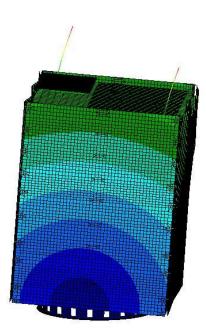
Figure 4: Mode shape of the reference main global mode of UPMSat-2 satellite without two opposite antennas
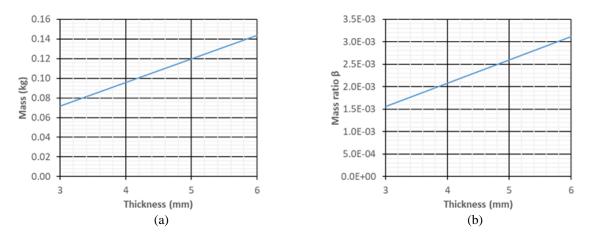

Figure 5: (a) Variation of the mass of two antennas with their thickness. (b) Variation of the mass ratio β with the thickness.
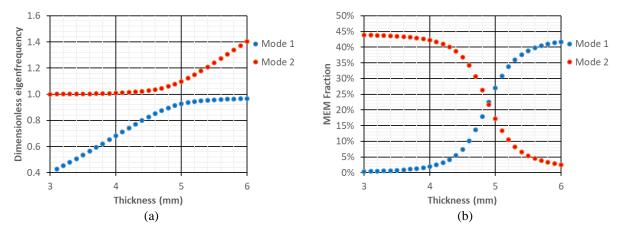

Figure 6: Variation of the numerical results with the thickness of the antennas: (a) Dimensionless eigenfrequencies. (b) Modal Effective Mass (MEM) Fractions.

Andrés García-Pérez, Marcos Chimeno Manguán, Ángel Sanz-Andrés and Gustavo Alonso

The results shown in this work have been obtained with the completed FEM of the satellite that includes the four antennas, where the thicknesses of the two selected antennas are varied from 3 mm to 6 mm with steps of 0.1 mm. The linear variation of the mass of these two antennas with their thicknesses can be seen in Figure 5(a). The mass ratio β is defined in [10] as the fraction between the masses of the secondary part and the primary part. In this case, the secondary part of the numerical model corresponds to the sum of the two studied antennas and the variation of β with respect to the thickness is linear, as can be seen in Figure 5(b). It can be observed that the mass fraction of both antennas with respect to the rest of the satellite is very low, with values ranging from 0.15% to 0.32%.

The dimensionless eigenfrequency parameter x_i described in [10] is the square of the ratio between one natural frequency f_i of the model and the reference natural frequency f_r, as is defined in the next equation.

$$x_i = \left(\frac{f_i}{f_r} \right)^2 \tag{1}$$

The evolution with the thickness of the two dimensionless eigenfrequencies of interest of the complete model and their associated MEM fractions are shown in Figure 6, where the variation step of the thickness is 0.1 mm. These two modes of interest are the global mode of the satellite in X direction and the first bending mode of the two antennas in the same direction. These results have been extracted from the normal modes analyses, where more modes are obtained from this complex model that are not taken into account in this work, but that may influence the presented results.

Both natural frequencies increase with the thicknesses of the antennas, where the frequency of the Mode 1 is always lower than that of the Mode 2. Particularly, the first dimensionless eigenfrequency is below the unit for all range of thickness values, while the second dimensionless eigenfrequency is above the unit, which is the minimum asymptotic limit for low thicknesses.

The dependency of the MEM fractions for both modes shown in Figure 6(b) indicates a monotonous increase of this value for the first mode and a monotonous decrease for the second mode. It is appreciated that there are three ranges of thickness values depending on the values and variations of the MEM fractions. It can be deduced that for the first range of thickness values, between 3 and 4.5 mm, the first mode corresponds to the local bending mode of the antennas with a MEM fraction below 10% and where the increment of the dimensionless eigenfrequency with the thickness presents a quasi linear trend. In this range, the second mode corresponds to the main global mode of the satellite with a MEM fraction value that decreases from 44 to 36%, but that is clearly higher than that of the first mode. The rest of the MEM fraction corresponds to the rest of modes of the model that are not taken into account in this study. There is a slight increment of the dimensionless eigenfrequency of the main mode in this first range as a consequence of the small effect of the modal coupling between the antennas and the primary structure. This effect will increase with the thickness due to the increment of the degree of modal coupling.

The second range of thickness values, which comprises from 4.6 to 5.2 mm, corresponds to the maximum degree of modal coupling between secondary and primary structure. One of the effects of the modal coupling is the higher variation of the MEM fractions for both modes compared to the other ranges. Precisely, with 4.9 mm, the values of the MEM fractions are practically the same between both modes, making it impossible to distinguish which is the local and which is the global one. Therefore, the main global mode that appeared for the first design range has been split into two similar global modes. One mode with a natural frequency below the reference one, and the second mode with a natural frequency above. This is one of the most interesting effects of the modal coupling, which in this example has been provoked by a secondary part with a practically negligible mass fraction compared to the entire satellite. There are also other effects on the structural results that will be discussed in the next section.

When the thickness of the antennas is higher than 5 mm, the MEM fraction of the first mode overpasses the MEM fraction of the second mode. From this design configuration, the modal behaviour is inverted and the first mode becomes the main global mode, while the second mode is still a global mode, but with a lower MEM fraction than that of the first mode and whose value decreases for higher thickness. For the third range of thickness values (5.3 – 6 mm), the MEM of the second mode is reduced below 10%, and therefore, it can be considered as the local bending mode of the antennas. In this case, the situation is similar to that of the first range, where there are one local mode and one global mode. The difference is that the natural frequency of the local mode is higher than that of the global mode in this third range.

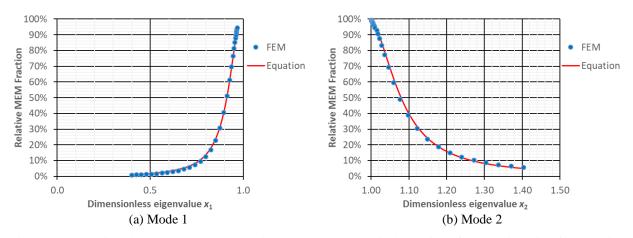(a) Mode 1   (b) Mode 2

Figure 7: Comparison between the FEM numerical results and analytical equation of the relationship of the relative MEM fraction with the dimensionless eigenfrequency

One of most interesting aspects observed in the numerical results is the relationship that exists between the obtained dimensionless eigenvalue x_i and the relative MEM fraction $m_{eff,rel,i}$ for the two considered modes. By comparing these numerical results with the analytical equations of the 2-DOF model (see Figure 7), it has been found that the numerical results follow with small deviation the next analytical equation extracted from [10], where a correction factor K_β that multiplies to the mass ratio β has been added in this work to match the numerical results.
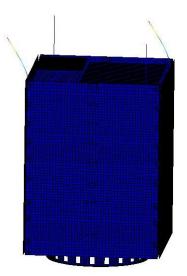
$$m_{eff,rel,i} = \frac{K_\beta \beta}{1 + K_\beta \beta} \frac{1}{K_\beta \beta x_i^2 + (1 - x_i)^2} \tag{2}$$

The relative mass fraction is defined as the ratio between the numerical MEM fraction of any of the modes and the sum of the MEM fractions of the two considered modes. The value for the correction factor K_β found for the first mode of this numerical model is 2.68, while for the second mode is 3. As can be seen in Figure 7, the curves calculated with Eq. (2) interpolate accurately the numerical results for both modes.
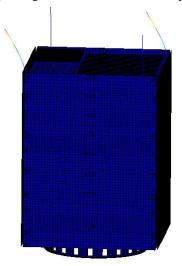
The mode shapes for the three different cases are shown in Figure 8. For the first case, with 3 mm of thickness, the first mode is clearly the local bending mode of the two considered antennas (Figure 8(a)), while the second mode is the global mode of the satellite (Figure 8(b)). These results agree with the solutions of the analytical 2-DOF model described in [10], where for the first mode, the motion of the secondary part is much higher than the primary mass, while for the second mode, the motions of both masses are similar in intensity but out of phase, as can also be appreciated in the FEM results shown in Figure 8(b). However, for the third case, the first mode is the global mode of the satellite (Figure 8(e)), where the motions of the secondary and primary parts are on phase and with similar intensity, while the second mode is the local mode of the secondary part (Figure 8(f)), with much more intensity on the motion of the antennas. These numerical results also agree the analytical solutions of the 2-DOF system described in [10].

The mode shapes for the situation of the maximum degree of modal coupling correspond to the design case where the thickness of the antennas is 4.9 mm. The first mode shape (Figure 8(c)) is similar to that of the second mode (Figure 8(d)), where the motions of the antennas are amplified to the maximum level as an effect of the modal coupling. This result agrees with the conclusion extracted from the 2-DOF system in [10], where the amplitude of the motion of the secondary mass is much higher than for the primary mass for both modes in the case of modal coupling, and where this difference of intensity is higher for lower values of the mass ratio β. Due to this fact, the motion of the primary structure cannot be appreciated in the FEM figures for this design case, but theoretically is in phase with the motion of the antennas for the first mode and out of phase for the second mode.
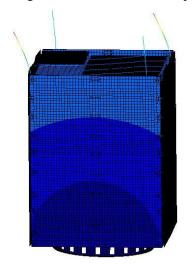
Andrés García-Pérez, Marcos Chimeno Manguán, Ángel Sanz-Andrés and Gustavo Alonso

(a) Design case: 3 mm. Mode 1 shape.

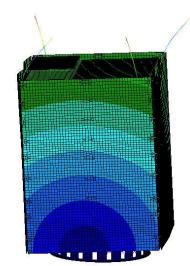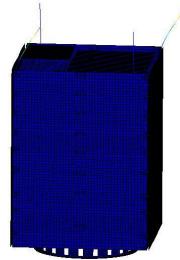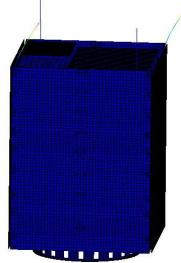(b) Design case: 3 mm. Mode 2 shape.

(c) Design case: 4.9 mm. Mode 1 shape.

(d) Design case: 4.9 mm. Mode 2 shape.

(e) Design case: 6 mm. Mode 1 shape.

(f) Design case: 6 mm. Mode 2 shape.

Figure 8: FEM mode shapes for different configurations

4.2 Sine vibration analyses

In this section, the numerical results obtained from the sine vibration analyses applied to the different proposed configurations of the UPMSat-2 FEM are presented. The vibration consists in a forced acceleration defined to a base node that is attached via a rigid element to all the interfaces nodes of the UPMSat-2 adaptor, transmitting the input acceleration to the structure of the satellite. The input acceleration is defined with a constant 0 – peak amplitude of 2.5 g between 5 to 130 Hz. The modal viscous damping for these analyses is a constant value of 0.02 for all the frequency range.

The results considered for this study are the maximum bending stresses calculated at the lower section of the antennas and the lateral forces in the global X direction obtained in the CBUSH elements that represent the interface bolts of the satellite. The bending stresses represent the most severe structural effect on the antennas, while the interface forces are appropriated results to evaluate the impact of the variation of the modal effective masses on the structural results of the main structure.

The variation of the lateral forces on the 20 interface elements are shown in Figure 9. These results are the 0 – peak amplitudes of the dynamic lateral forces calculated when the frequency of the excitation corresponds to the natural frequency of the global mode in each design case, that is to say, of the mode with the highest value of MEM fraction. The differences in the forces among these elements depend on their location with respect to the direction of the input acceleration. For all elements, the maximum force is reached for the minimum considered thickness of 3 mm. The forces decrease as the degree of modal coupling becomes higher and reach their minimum value just at the design point when the degree of modal coupling is maximum, with a thickness value of 4.9 mm. From this point, there is a change in the trend and the forces increase for higher values of thickness due to the reduction of the degree of the modal coupling. The comparison between the maximum and minimum values of these interface forces is shown in Table 1. The modal coupling of the antennas achieves a reduction between 57.1 and 63.7% of these values, which is a remarkable conclusion taking into account the small mass of the antennas compared to the entire satellite. From this point of view, the modal coupling seems to be a positive effect for the main structure because it achieves a reduction of the maximum loads supported by the interface bolts, which in turn decreases the risk of bolt failures. But it has also its negative consequences such as the increment of the bending stresses generated in the base sections of the affected antennas, as can be seen in the curve depicted in Figure 10. In this graph, the amplitude of the bending stress increase initially with the thickness due to that the effect of having a higher degree of modal coupling is more influential than the fact of having a more rigid beam. The maximum stress is reached for the design case of 4.9 mm of thickness, which coincides with the maximum degree of modal coupling. Then, the stress decreases with the thickness due to combined effect of reducing the degree of modal coupling and the increase of the rigidity of the antennas. Taking into account that the tensile strength limit of the antennas material (copper – beryllium alloy) is about 330 MPa, it is probable a mechanical failure of these elements under the considered sine vibration excitation for the configurations from 3.8 to 5.9 mm of thickness. Therefore, from the secondary part point of view, the modal coupling is an undesirable effect that can provoke the break of these elements and, thus, must be avoided.
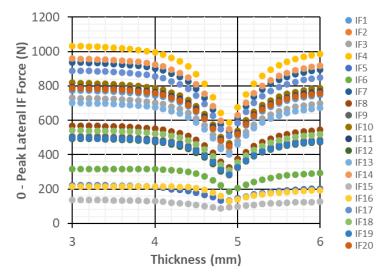

Figure 9: Variation of the lateral forces on the interface elements with the thickness of the antennas

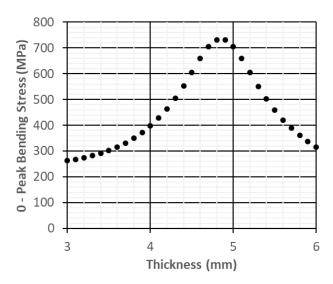Andrés García-Pérez, Marcos Chimeno Manguán, Ángel Sanz-Andrés and Gustavo Alonso

Figure 10: Variation of the maximum bending stress on the lower section of the antennas with their thickness

Table 1: Comparison of the maximum and minimum interface forces obtained from sine vibration analyses

| IF | 0 – Peak Lateral Force (N) | | Max – Min |
	Maximum	Minimum	Ratio
IF1	774	444	57.3%
IF2	494	282	57.1%
IF3	730	417	57.1%
IF4	1031	589	57.1%
IF5	222	132	59.4%
IF6	317	185	58.2%
IF7	937	534	57.0%
IF8	569	326	57.3%
IF9	507	291	57.3%
IF10	818	468	57.2%
IF11	793	455	57.3%
IF12	494	282	57.2%
IF13	702	402	57.3%
IF14	958	550	57.4%
IF15	137	87	63.7%
IF16	216	130	60.1%
IF17	889	509	57.2%
IF18	541	311	57.6%
IF19	496	285	57.5%
IF20	786	450	57.2%

5. Conclusions

The effects of the modal coupling between a secondary element and the primary structure have been studied in this work with the numerical model of the UPMSat-2 satellite. The results calculated from the normal modes analyses and sine vibration simulations have allowed the investigation of this phenomenon in a case where small components can remarkably change the dynamic behaviour of the entire system. In particular, the secondary elements are two communication antennas located vertically like cantilevered beams at the top of the satellite and whose masses do not overpass the 1% of the mass of the satellite. In spite of this very small mass fraction of the antennas, they can substantially modify the structural parameters of the entire system, such as the natural frequencies and their associated modal effective masses, to the point of converting one global mode into two global modes for the case of maximum degree of modal coupling. The numerical results exposed in this paper have been compared with the analytical equations of the undamped 2-DOF system showing similarities between both approaches. This agreement is interesting

to validate the analytical approach in the evaluation of the modal coupling of space systems in the early design phases, when a detailed model is not available.

Other structural results are also affected due to the modal coupling, such as the forces generated on the interface elements under a sine vibration load, which in the UPMSat-2 model are reduced about 57% with the maximum degree of modal coupling. These results show the benefits of the modal coupling on the main structure, but it has also its negative consequences for the secondary parts. In the example presented in this paper, these negative effects are materialized in the increment of the maximum bending stresses generated in the antennas that exceed their maximum allowable limit, which in turn can provoke the structural collapse of these elements.

Therefore, it is important to take into account all these effects, both positive and negative, of the modal coupling for the mechanical design of space systems. These structures will be subjected to intense dynamic loads, especially during the launch phase, which will generate high forces and stresses in all involved components. Depending of the dynamic design of these systems, these forces and stresses can be intensified or mitigated. Modal coupling is an important aspect that must also be taken into account due to its determining influence on these structural responses.

Acknowledgements

References

[1] J.J. Wijker. 2008. Spacecraft Structures. Springer Berlin Heidelberg, Berlin, Heidelberg.

[2] ECSS. 2013., ECSS-E-HB-32-26A, Space engineering, Spacecraft mechanical loads analysis handbook. ESA-ESTEC Requirements and Standards Division, Noordwijk, The Netherlands.

[3] J.P. Den Hartog. 1947. Mechanical Vibrations. Third Edit, McGraw-Hill Book Company, Inc, New York and London.

[4] R. Rana, T.T. Soong. 1998. Parametric study and simplified design of tuned mass dampers. *Eng. Struct*. 20:193–204.

[5] T. Taniguchi, A. Der Kiureghian, M. Melkumyan. 2008. Effect of tuned mass damper on displacement demand of base-isolated structures. *Eng. Struct*. 30:3478–3488.

[6] C.C. Lin, L.Y. Lu, G.L. Lin, T.W. Yang. 2010. Vibration control of seismic structures using semi-active friction multiple tuned mass dampers. *Eng. Struct*. 32:3404–3417.

[7] A.A. Farghaly, M. Salem Ahmed. 2012. Optimum Design of TMD System for Tall Buildings. *ISRN Civ. Eng*. 1–13.

[8] E. Pascale, P. Eccleston, G. Tinetti. 2018. The ARIEL Space Mission. In: *2018 5th IEEE Int. Work. Metrol. Aerosp., IEEE*. 31–34.

[9] L. Liu, J. Shan, Y. Zhang. 2016. Dynamics Modeling and Analysis of Spacecraft with Large Deployable Hoop-Truss Antenna.. *J. Spacecr. Rockets*. 53:471–479.

[10] A. García-Pérez, Á. Sanz-Andrés, G. Alonso, M. Chimeno Manguán. 2019. Dynamic coupling on the design of space structures. *Aerosp. Sci. Technol*. 84:1035–1048.

[11] S. Pindado, E. Roibas-Millan, J. Cubas, A. Garcia, A. Sanz, S. Franchini, I. Perez-Grande, G. Alonso, J. Perez-Alvarez, F. Sorribes-Palmer, A. Fernandez-Lopez, M. Ogueta-Gutierrez, I. Torralbo, J. Zamorano, J.A. de la Puente, A. Alonso, J. Garrido. 2017. The UPMSat-2 Satellite : An Academic Project within Aerospace Engineering Education. *Atiner Conf. Pap. Ser. (2017)*.

[12] S. Pindado, J. Cubas, E. Roibás-Millán, F. Sorribes-Palmer. 2018. Project-based learning applied to spacecraft power systems: a long-term engineering and educational program at UPM University. *CEAS Sp. J*. 10:307–323.

[13] J. Cubas, A. Farrahi, S. Pindado. 2015. Magnetic Attitude Control for Satellites in Polar or Sun-Synchronous Orbits. *J. Guid. Control. Dyn*. 38:1947–1958.

[14] J. Zamorano, J. Garrido, J. Cubas, A. Alonso, J.A. de la Puente. 2017. The Design and Implementation of the UPMSAT-2 Attitude Control System. *IFAC-PapersOnLine*. 50:11245–11250.

[15] E. Rodríguez-Rojo, S. Pindado, J. Cubas, J. Piqueras-Carreño. 2019. UPMSat-2 ACDS magnetic sensors test campaign. *Measurement*. 131:534–545.

[16] E. Roibás-Millán, A. Alonso-Moragón, A.G. Jiménez-Mateos, S. Pindado. 2017. Testing solar panels for small-size satellites: the UPMSAT-2 mission. *Meas. Sci. Technol*. 28:115801.

[17] Á. Porras-Hermoso, S. Pindado, J. Cubas. 2018. Measurement Science and Technology Lithium-ion battery performance modeling based on the energy discharge level Lithium-ion battery performance modeling based on the energy discharge level. *Meas. Sci. Technol*. 29:1–6.

[18] J. Garrido, J. Zamorano, A. Alonso, J.A. de la Puente. 2018. Timing Analysis of the UPMSat-2 Communications Subsystem. *IFAC-PapersOnLine*. 51:217–222.